Andreas Prestel | Heiko M. Möller

Spatio-temporal control of cellular uptake achieved by photoswitchable cell-penetrating peptides

Suggested citation referring to the original publication:
Chem. Commun. 52 (2015) 701–704
DOI http://dx.doi.org/10.1039/C5CC06848G

ChemComm

COMMUNICATION

View Article Online
View Journal | View Issue

Cite this: *Chem. Commun.*, 2016, **52**, 701

Received 14th August 2015,
Accepted 30th October 2015

DOI: 10.1039/c5cc06848g

www.rsc.org/chemcomm

Spatio-temporal control of cellular uptake achieved by photoswitchable cell-penetrating peptides†

Andreas Prestel[a] and Heiko M. Möller*[ab]

The selective uptake of compounds into specific cells of interest is a major objective in cell biology and drug delivery. By incorporation of a novel, thermostable azobenzene moiety we generated peptides that can be switched optically between an inactive state and an active, cell-penetrating state with excellent spatio-temporal control.

Cell-penetrating peptides (CPPs) are mostly polycationic and/or amphiphilic peptides with the ability to cross the hydrophobic cellular membrane.[1–3] The exact mechanism of cellular uptake is still a subject of scientific discourse and there are controversial results, indicating different mechanisms, depending on the type of CPP and experimental conditions.[4–6] Nevertheless, these vectors are widely used to deliver various cargos into living cells, including small molecules, macromolecules like proteins or oligonucleotides, as well as nanoparticles and liposomes.[7–9] Since these peptides enter cells rather unspecifically, much effort has been made towards a selective uptake into specific cells of interest. To this end, the peptides remain in an inactive state until exposed to an external trigger like heat,[11] pH[12] or light-induced deprotection.[13] Prominent members in the group of cationic CPPs are oligoarginines (Arg_8, Arg_9), which are commonly used for membrane translocation.[14,15] It has been shown that their cellular uptake can be inhibited by masking the positively charged guanidinium groups of arginines using polyanionic structures like heparin.[16] This was used to design activatable CPPs (ACPPs), in which the oligoarginine is linked to a polyanionic peptide *via* a cleavable turn-structure.[17] Upon scission of the linker by specific proteases or other external factors, the polyanions dissociate and the polycationic peptides are released to deliver their cargo into the cells.[17–19] These ACPP allow for controlling cellular uptake in temporal fashion. However, the spatial control is rather limited because of the diffusion of the activating reagent. Furthermore, activation of ACPPs is one-way and there is no handle to deactivate these structures.

An interesting possibility to control the function of biomolecules reversibly is the incorporation of azobenzene (AB) moieties.[20–23] AB can adopt two distinct configurations of its central N=N-bond (*cis* and *trans*), which can be interconverted by irradiation at appropriate wavelengths[24] and the photochemical properties can be tuned by altering the substitution pattern.[25] In the dark, the energetically favoured *trans*-AB is almost exclusively formed and it adopts a nearly planar conformation. Upon irradiation it can be converted into the *cis*-AB with a twisted arrangement of its benzene moieties. A photostationary state (PSS) is reached where, depending on the wavelength, either the *cis*-AB ($\lambda \approx 360$ nm) or the *trans*-AB ($\lambda \approx 440$ nm) is the predominant form.[26] To reversibly control the function of peptides with ABs, two major principles have been reported: either cyclization *via* side chains[27] or incorporation into the peptide backbone.[28] In the latter case the twisted *cis*-AB is mostly used to mimic a native β-turn, while the linear, extended *trans*-AB prevents β-turn formation.[29]

Here, we describe the synthesis of a photoswitchable CPP (PCPP) comprised of a cell-penetrating oligoarginine linked to an inhibitory oligoglutamate by an AB moiety, which is integrated into the peptide backbone. In the *cis*-form, the AB adopts a turn-like structure and allows for an efficient pairing of the two oppositely charged peptide sequences, whereas the extended *trans*-form is supposed to disrupt this pairing, release the oligoarginine and, consequently, induce cellular uptake (Scheme 1). In order to slow down thermal *cis-to-trans* isomerization, methyl substituents in *ortho*-position were introduced.[30,31] To maximize the spatial rearrangement and reduce any internal flexibility, an AB was chosen that yields very rigid aromatic amides in *para* position after incorporation into the peptide backbone.

The synthesis of the AB-moiety (**2**) is outlined in Scheme 2a. To avoid the difficult coupling of the aromatic amine during solid phase peptide synthesis (SPPS), the first glutamate residue was attached in solution to yield compound **3**, which could be coupled quantitatively in the next step. To monitor cellular uptake, the N-terminus of the peptides was modified with a

[a] *Department of Chemistry and Konstanz Research School Chemical Biology, University of Konstanz, 78464 Konstanz, Germany*
[b] *Institute of Chemistry/Analytical Chemistry, University of Potsdam, 14476 Potsdam, Germany. E-mail: heiko.moeller@uni-potsdam.de*

† Electronic supplementary information (ESI) available. See DOI: 10.1039/c5cc06848g

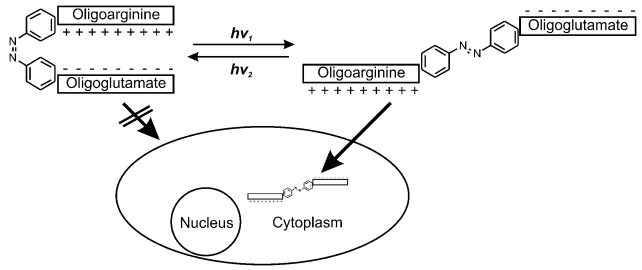

Scheme 1 Principle of photoswitchable cell penetrating peptides.

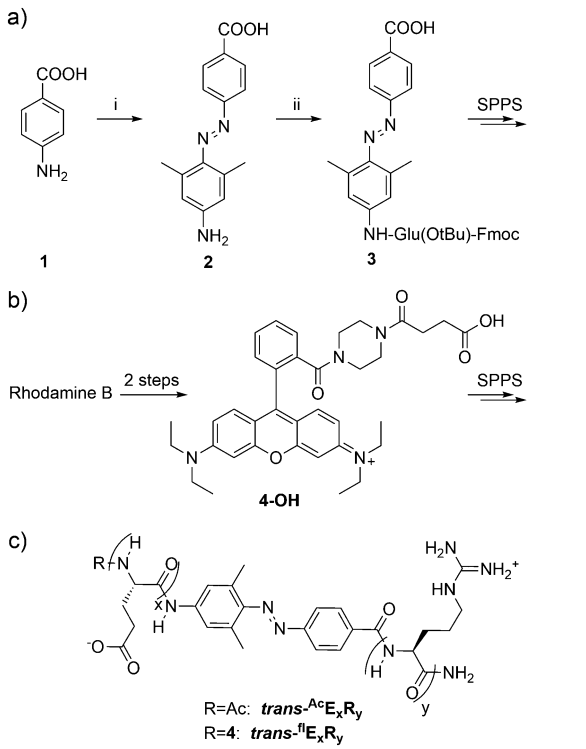

Scheme 2 (a) Synthesis of the AB moiety. Reagents and conditions: (i) $NaNO_2$, $HCl_{aq.}$, 0 °C, 30 min, then 3,5-dimethylaniline, 0 °C, 2 h, 70%; (ii) Fmoc-Glu(O^tBu)-OH, HATU, HOAt, DIPEA, NMP, 23 °C, 14 h. (b) Compound **4-OH** was used for fluorescent labelling of the peptides and synthesized according to Nguyen *et al.* from Rhodamine B in 2 steps.[10] (c) Structure of the PCPPs used in this study. The nomenclature of the peptides was defined as follows: the configuration of the AB moiety is denoted by the prefix '*cis*' or '*trans*'. The fluorescently labelled peptides are indicated by a superscripted 'fl', the acetylated peptides by 'Ac'. The number of consecutive glutamate and arginine residues is specified by $\mathbf{E_xR_y}$. Three different chain lengths were investigated: $x = 6$ $y = 9$; $x = y = 8$ and $x = y = 9$.

rhodamine dye (**4-OH**), which was prepared from rhodamine B as previously described by Nguyen *et al.*[10] The peptides were synthesized on solid support and purification was achieved *via* RP-HPLC (for experimental details see ESI†). Three different peptides ($\mathbf{E_6R_9}$, $\mathbf{E_8R_8}$ and $\mathbf{E_9R_9}$; see Scheme 2c) were synthesized based on the design by Jiang *et al.*[17] to investigate the influence of chain length on cellular uptake and other biophysical properties like solubility. The *cis*-peptides were generated by irradiation at 366 nm. After about 5 minutes a photostationary state was established, with 30–80% of the peptide converted, depending on peptide sequence and experimental conditions (solvent, pH). Irradiation at 438 nm or 495 nm reversed the isomerization and the initial state of almost 100% *trans*-peptide was recovered (Fig. 1a). However, the *cis*-peptides could be isolated by RP-HPLC using shallow gradients. In Fig. 1b consecutive UV/Vis-spectra of $^{Ac}\mathbf{E_6R_9}$ are displayed, illustrating the thermal *cis*-to-*trans* relaxation. It is evident that the *cis*-peptide obtained after RP-HPLC is quite pure (>95%) and that the thermal isomerization is sufficiently slow, with a half-life of about 30 hours at 22 °C. This photochemical behaviour is representative for all peptides and conditions used in this study (for details see Fig. S2, ESI†). That the *cis*-peptide indeed adopts a turn-like structure could be shown by NMR spectroscopy revealing NOE contacts between side chain HN groups of Arg and H^{β} and H^{γ} of Glu (Fig. S3, ESI†). The cellular uptake of the two isomers was investigated by confocal microscopy. In Fig. 2 the uptake of ***cis***- and ***trans***-$^{fl}\mathbf{E_9R_9}$ into HeLa-cells is visualized. After 40, 90 and 135 minutes the *cis*-form was only taken up marginally (Fig. 2a, c and e), while the *trans*-form accumulated rapidly in the cytoplasm of the cells (Fig. 2f, Fig. S4 and S5, ESI†). To convert the *cis*-into the activated *trans*-peptide, a region of interest was irradiated at 488 nm with high laser intensity (240 μW; ~0.4 ms μm^{-2}) under the confocal microscope. During the following incubation period, the peptide was taken up by the cells at comparable levels as achieved by direct addition of the *trans*-peptide (Fig. 2b and d; supplementary movies, ESI†). Using the spatially restricted confocal laser beam, selected areas on the same dish could be activated while distant areas were unaffected. To quantify the uptake, the incubated cells were additionally analyzed by flow cytometry. While the *trans*-form of all 3 investigated peptides entered HeLa-cells very efficiently, the respective *cis*-peptide was taken up to a much lesser extent and inhibition was most effective for ***cis***-$^{fl}\mathbf{E_9R_9}$ (Fig. 2g, Fig. S6, ESI†). This light triggered translocation of the peptides could also be shown for 4 other cell lines (HCT116, BSC1, MCF7 and RPE1), documenting the broad applicability of the PCPPs (Fig. S5, ESI†). In all cases, the activated peptides show an inhomogeneous distribution in the cytoplasm of the cells (Fig. S4, ESI†). It should be noted here that a significant portion of the activated CPP might not be

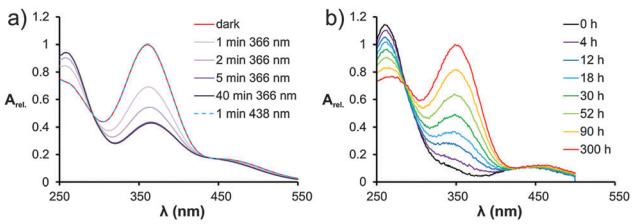

Fig. 1 (a) Photoswitching properties of $^{Ac}\mathbf{E_6R_9}$ in water at 22 °C. In the dark, the *trans*-form of AB gives rise to a strong absorption band at 355 nm (red curve). Upon irradiation at 366 nm, A_{355} drops and a PSS is reached after about 5 minutes (shaded purple curves). This effect is reversed when irradiating at 438 nm (dashed blue curve on top of the red curve). (b) Thermal *cis*-to-*trans* isomerization of $^{Ac}\mathbf{E_6R_9}$ monitored by consecutive UV/Vis-spectra. The black spectrum is obtained directly after elution from RP-HPLC and corresponds to almost pure *cis*-form (95.6% *cis*-form, see also Fig. S1 of the ESI†). The half-life of thermal isomerization is about 30 h (21% MeCN; 0.1% TFA in water, 22 °C).

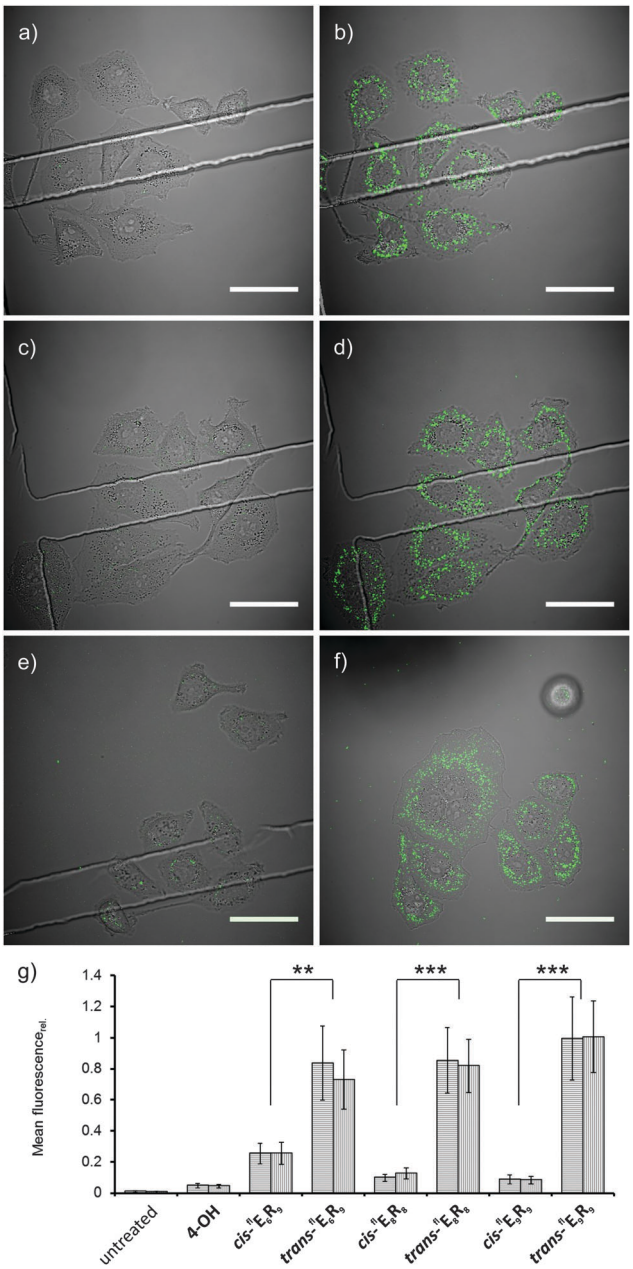

Fig. 2 Peptide uptake into HeLa-cells monitored by confocal microscopy and flow cytometry. (a–f) Merged fluorescence (green) and bright field (grayscale) images (scale bar: 50 μm). (a–e) Sequential activation of different regions on the same dish. Cells incubated with 1 μM ***cis*-^{fl}E$_9$R$_9$** for 40, 90 and 135 minutes, respectively, without activation (a, c and e) and 40 minutes after activation by irradiation at 488 nm; 240 μW; ~0.4 ms μm^{-2} (b and d). (f) Cells incubated directly with 1 μM ***trans*-^{fl}E$_9$R$_9$** for 65 minutes. (g) Mean fluorescence (relative to ***trans*-^{fl}E$_9$R$_9$**) per cell analyzed by flow cytometry. HeLa-cells were incubated with 3 μM of the respective peptide for 30 minutes. Two independent experiments per compound with >4000 cells each. Error bars give the standard-deviation of an individual experiment, wherein ~68% of the observed cells are represented. The significance was assessed using an unpaired *t*-test (**: $p < 0.01$; ***: $p < 0.001$).

internalized but enriched at the plasma membrane.[32] These membrane-bound CPPs might remain undetected due to fluorescence quenching.

The intracellular distribution is indicative of a vesicular uptake mode in accordance to many reports of substituted oligoarginines.[33,34] This reduces the bioavailability of the delivered compound but several endosomal escape or cleavage mechanisms are described in literature.[35,36]

When irradiated with a single beam of high laser intensity, the spatial resolution is limited, because peptides in a large volume above the confocal plane are also activated and can diffuse quickly to regions several 100 μm away (Fig. 3a). However, by applying strongly reduced laser intensity (1 to 1.5 μW) in a repeated fashion we were able to achieve spatially restricted uptake into a few (1–5) selected cells, while neighboring cells were only barely affected (Fig. 3b and c).

Using an azobenzene building block offers the possibility to not only photo-activate cellular uptake but also to switch the CPP back into the inactive state. Indeed, the acetylated peptide **^{Ac}E$_9$R$_9$** could be switched back to the inactive, *cis*-form with 80% yield (Fig. S1, ESI†) by irradiation with UV-light (~360 nm). Similar switching yields should be achievable with many different cargos. However, when attaching a fluorescent dye it is known that the *trans*-to-*cis* conversion yield is significantly reduced, in case of **^{fl}E$_9$R$_9$** to ~40% (compare RP-HPLC runs in Fig. S1, ESI†) This phenomenon was previously described for other peptides containing an AB photoswitch and different fluorophores, but the exact mechanisms for the shift of the equilibrium at the photostationary state are not known.[37]

When using caged compounds or photodeprotection there is at least a risk of toxicity or unwanted side effects caused by the released caging groups. In our case, we are, first, able to prevent uptake in areas that have not been irradiated, and, second, there is no release of a caging group. No toxic effect was observable using the fluorescent peptides at low micromolar concentrations in cell culture. To further evaluate the toxicity, an alamar blue® assay was performed, but no impact on cell proliferation was detected even after prolonged exposure at

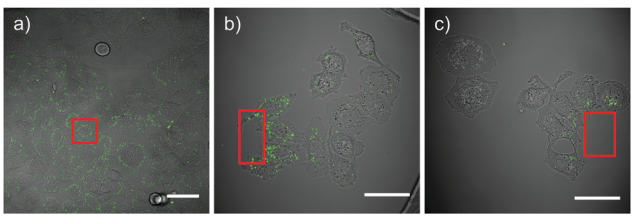

Fig. 3 Spatial control of cellular uptake by local activation of PCPPs. Merged fluorescence (green) and bright field (grayscale) images (scale bar: 50 μm). (a) After addition of ***cis*-^{fl}E$_9$R$_9$** (3 μM), the highlighted area (red box) was irradiated with high laser intensity (488 nm; 200 μW; ~60 ms μm^{-2}) and the picture was taken after 30 minutes of incubation. (b) After addition of ***cis*-^{fl}E$_9$R$_9$** (1 μM), the highlighted area (red box) was irradiated with reduced laser intensity (488 nm; 1.5 μW; ~60 ms μm^{-2}). Irradiation was repeated every minute for 30 minutes and the picture was taken after 10 additional minutes of incubation. (c) After addition of ***cis*-^{fl}E$_9$R$_9$** (1 μM), the highlighted area (red box) was irradiated with reduced laser intensity (488 nm; 1 μW; ~60 ms μm^{-2}). Irradiation was repeated every minute for 20 minutes and the picture was taken after 20 additional minutes of incubation. To avoid complications arising from irradiating a volume located within the cells we positioned the activated volume directly adjacent to a group of cells.

concentrations up to 40 μM (Fig. S7, ESI†). To our knowledge, this is the first report of a photoswitchable cell penetrating peptide and this vector could be used to deliver various conjugated cargos to selected cells with excellent spatial and temporal resolution.

We would like to thank Prof. Dr T. U. Mayer and A. Brendel (cell culture); Prof. Dr M. Groettrup and Dr M. Basler (flow cytometry) as well as Prof. Dr E. May and D. Hermann (confocal microscopy at the Bioimaging Center of the University of Konstanz) for their expertise, and infrastructural support. Financial support through the University of Konstanz is gratefully acknowledged. We would like to thank Prof. Dr V. Wittmann for critically reading the manuscript.

Notes and references

1 A. D. Frankel and C. O. Pabo, *Cell*, 1988, **55**, 1189–1193.
2 J. P. Richard, K. Melikov, E. Vives, C. Ramos, B. Verbeure, M. J. Gait, L. V. Chernomordik and B. Lebleu, *J. Biol. Chem.*, 2003, **278**, 585–590.
3 M. Lindgren, M. Hällbrink, A. Prochiantz and Ü. Langel, *Trends Pharmacol. Sci.*, 2000, **21**, 99–103.
4 F. Madani, S. Lindberg, U. Langel, S. Futaki and A. Graslund, *J. Biophys.*, 2011, **2011**, 414729.
5 F. Milletti, *Drug Discovery Today*, 2012, **17**, 850–860.
6 S. Stalmans, E. Wynendaele, N. Bracke, B. Gevaert, M. D'Hondt, K. Peremans, C. Burvenich and B. De Spiegeleer, *PLoS One*, 2013, **8**, e71752.
7 S. T. Henriques, M. N. Melo and M. A. Castanho, *Biochem. J.*, 2006, **399**, 1–7.
8 F. Heitz, M. C. Morris and G. Divita, *Br. J. Pharmacol.*, 2009, **157**, 195–206.
9 N. Nischan, H. D. Herce, F. Natale, N. Bohlke, N. Budisa, M. C. Cardoso and C. P. R. Hackenberger, *Angew. Chem., Int. Ed.*, 2015, **54**, 1950–1953.
10 T. Nguyen and M. B. Francis, *Org. Lett.*, 2003, **5**, 3245–3248.
11 R. L. Bartlett, 2nd, S. Sharma and A. Panitch, *Nanomedicine*, 2013, **9**, 419–427.
12 E. Jin, B. Zhang, X. Sun, Z. Zhou, X. Ma, Q. Sun, J. Tang, Y. Shen, E. Van Kirk, W. J. Murdoch and M. Radosz, *J. Am. Chem. Soc.*, 2013, **135**, 933–940.
13 Y. Shamay, L. Adar, G. Ashkenasy and A. David, *Biomaterials*, 2011, **32**, 1377–1386.
14 S. Futaki, T. Suzuki, W. Ohashi, T. Yagami, S. Tanaka, K. Ueda and Y. Sugiura, *J. Biol. Chem.*, 2001, **276**, 5836–5840.
15 D. M. Copolovici, K. Langel, E. Eriste and U. Langel, *ACS Nano*, 2014, **8**, 1972–1994.
16 S. M. Fuchs and R. T. Raines, *Biochemistry*, 2004, **43**, 2438–2444.
17 T. Jiang, E. S. Olson, Q. T. Nguyen, M. Roy, P. A. Jennings and R. Y. Tsien, *Proc. Natl. Acad. Sci. U. S. A.*, 2004, **101**, 17867–17872.
18 R. Weinstain, E. N. Savariar, C. N. Felsen and R. Y. Tsien, *J. Am. Chem. Soc.*, 2014, **136**, 874–877.
19 M. Whitney, E. N. Savariar, B. Friedman, R. A. Levin, J. L. Crisp, H. L. Glasgow, R. Lefkowitz, S. R. Adams, P. Steinbach, N. Nashi, Q. T. Nguyen and R. Y. Tsien, *Angew. Chem., Int. Ed.*, 2013, **52**, 325–330.
20 A. A. Beharry and G. A. Woolley, *Chem. Soc. Rev.*, 2011, **40**, 4422–4437.
21 M. Schönberger and D. Trauner, *Angew. Chem., Int. Ed.*, 2014, **53**, 3264–3267.
22 T. Fehrentz, M. Schönberger and D. Trauner, *Angew. Chem., Int. Ed.*, 2011, **50**, 12156–12182.
23 L. Nevola, A. Martín-Quirós, K. Eckelt, N. Camarero, S. Tosi, A. Llobet, E. Giralt and P. Gorostiza, *Angew. Chem.*, 2013, **125**, 7858–7862.
24 G. S. Hartley, *Nature*, 1937, **140**, 281.
25 O. Sadovski, A. A. Beharry, F. Zhang and G. A. Woolley, *Angew. Chem., Int. Ed.*, 2009, **48**, 1484–1486.
26 W. R. Brode, J. H. Gould and G. M. Wyman, *J. Am. Chem. Soc.*, 1952, **74**, 4641–4646.
27 J. R. Kumita, O. S. Smart and G. A. Woolley, *Proc. Natl. Acad. Sci. U. S. A.*, 2000, **97**, 3803–3808.
28 A. Cattani-Scholz, C. Renner, C. Cabrele, R. Behrendt, D. Oesterhelt and L. Moroder, *Angew. Chem., Int. Ed.*, 2002, **41**, 289–292.
29 C. Hoppmann, S. Seedorff, A. Richter, H. Fabian, P. Schmieder, K. Rück-Braun and M. Beyermann, *Angew. Chem.*, 2009, **121**, 6763–6766.
30 H. Nishioka, X. Liang and H. Asanuma, *Chem. – Eur. J.*, 2010, **16**, 2054–2062.
31 M. R. Han, D. Hashizume and M. Hara, *New J. Chem.*, 2007, **31**, 1746–1750.
32 A. Walrant, I. Correia, C.-Y. Jiao, O. Lequin, E. H. Bent, N. Goasdoué, C. Lacombe, G. Chassaing, S. Sagan and I. D. Alves, *Biochim. Biophys. Acta, Biomembr.*, 2011, **1808**, 382–393.
33 T. Tsumuraya and M. Matsushita, *PLoS One*, 2014, **9**, e86639.
34 S. M. Fuchs and R. T. Raines, *Biochem. J.*, 2004, **43**, 2438–2444.
35 H. Fuchs, C. Bachran and D. Flavell, *Antibodies*, 2013, **2**, 209–235.
36 A. K. Varkouhi, M. Scholte, G. Storm and H. J. Haisma, *J. Controlled Release*, 2011, **151**, 220–228.
37 A. A. Beharry, L. Wong, V. Tropepe and G. A. Woolley, *Angew. Chem., Int. Ed.*, 2011, **50**, 1325–1327.

